

This article was downloaded by: [Siauliu University Library]

On: 17 February 2013, At: 07:26

Publisher: Taylor & Francis

Informa Ltd Registered in England and Wales Registered Number: 1072954

Registered office: Mortimer House, 37-41 Mortimer Street, London W1T 3JH, UK



## Advanced Composite Materials

Publication details, including instructions for authors and subscription information:

<http://www.tandfonline.com/loi/tacm20>

### On the shape control of environmentally responsive composite with embedded Ti-Ni alloy as effectors

Hitoshi Yoshida <sup>a</sup>, Atsuo Funaki <sup>b</sup> & Shoichiro Yano <sup>c</sup>

<sup>a</sup> National Institute of Materials and Chemical Research (NIMC), 1-1, Higashi, Tsukuba, Ibaraki, 305 Japan

<sup>b</sup> Mie Industrial Research Institute, 3485, Ohtsuka, Takachayakomoricho, Tsu, Mie, 514 Japan

<sup>c</sup> National Institute of Materials and Chemical Research (NIMC), 1-1, Higashi, Tsukuba, Ibaraki, 305 Japan

Version of record first published: 02 Apr 2012.

To cite this article: Hitoshi Yoshida, Atsuo Funaki & Shoichiro Yano (1997): On the shape control of environmentally responsive composite with embedded Ti-Ni alloy as effectors, *Advanced Composite Materials*, 6:4, 341-352

To link to this article: <http://dx.doi.org/10.1163/156855197X00184>

PLEASE SCROLL DOWN FOR ARTICLE

Full terms and conditions of use: <http://www.tandfonline.com/page/terms-and-conditions>

This article may be used for research, teaching, and private study purposes. Any substantial or systematic reproduction, redistribution, reselling, loan, sub-licensing, systematic supply, or distribution in any form to anyone is expressly forbidden.

The publisher does not give any warranty express or implied or make any representation that the contents will be complete or accurate or up to date. The accuracy of any instructions, formulae, and drug doses should be independently verified with primary sources. The publisher shall not be liable for any loss, actions, claims, proceedings, demand, or costs or damages whatsoever or



howsoever caused arising directly or indirectly in connection with or arising out of the use of this material.



## On the shape control of environmentally responsive composite with embedded Ti–Ni alloy as effectors

HITOSHI YOSHIDA,<sup>1</sup> ATSUO FUNAKI<sup>2</sup> and SHOICHIRO YANO<sup>1</sup>

<sup>1</sup>National Institute of Materials and Chemical Research (NIMC), 1-1, Higashi, Tsukuba, Ibaraki, 305 Japan

<sup>2</sup>Mie Industrial Research Institute, 3485, Ohtsuka, Takachayakomoricho, Tsu, Mie, 514 Japan

Received 13 February 1996; accepted 29 May 1996

**Abstract**—Responsive shape control of Environmentally Responsive Composites (ERCs) composed of Ti–Ni alloy effectors and CFRTP (Carbon Fiber Reinforced Thermoplastic) was investigated. The responsive shape of the ERC was controlled by means of curvature control. When the material properties and initial curvature of the effectors are given and any curvatures of ERC specimen at low and high temperatures are designed, the initial curvature and flexural rigidity of the matrix could be calculated. Specimens of ERC were made from effectors and a matrix in which the initial curvature and flexural rigidity were the values calculated. Comparison was made between the designed values and the experimental values of curvature of the ERC specimens at low and high temperatures. As the results, the experimental values agreed fairly well with the designed values. It was shown that responsive shape control, which is a practically important factor, was possible.

**Keywords:** Smart materials; Ti–Ni alloy; environmentally responsive composite; shape control; bi-directional response; radius of curvature.

### 1. INTRODUCTION

Environmentally responsive materials are drawing attention as the next generation of materials and intensive research efforts have been made in this area. Environmentally responsive materials are called ‘smart materials’ or ‘intelligent materials’ and are defined as those materials that possess sensor functions to sense environmental conditions, an effector function as a power source to alter the shape and characteristics of the material, and a processor function to activate both the sensor and the effector functions by linking them to either outside or inside of the material. Noting that the force generated from Ti–Ni shape memory alloys is significantly different at low temperature and at high temperature, an environmentally responsive composite material was fabricated to possess bi-directional responses by compositizing them with a matrix phase. This new environmentally responsive composite material (called ERC thereafter) temporarily stores part of the large energy generated from Ti–Ni shape



memory alloys at high temperature as strain energy in the matrix and the bi-directional response characteristics can be realized by utilizing as the energy to restore the original shape. We have been developing a theory for tensile/compressive responses, flexural responses and torsional responses and the ‘responsiveness rate’ and the ‘recovery rate’ have been defined as the indices to represent the response characteristics. ERC specimens were fabricated by compositizing Ti–Ni shape memory alloys with matrices which have been reported in [1–4]. In this paper, the shape control necessary for the design of ERC as a practical engineering material has been investigated and examined. This investigation was carried out when the characteristics values of the effector were given and it was found that by appropriately selecting the characteristic values of the matrix, the shape of ERCs can be controlled at will at both low and high temperatures and thus highly practical ERCs can be realized.

2. CONTROL THEORY OF RESPONSIVE SHAPE OF ERC

The responsiveness rate and the recovery rate of ERC have been examined for the three types of responses of tensile/compressive responses, flexural responses and torsional responses [1–4]. In this paper, the method to control the responsive shape for the flexural response type ERC was examined which has better responsiveness and recovery rates and is most practical. As the responsive shape can be controlled by designing the curvature of ERC at high temperature and at low temperature, the following analysis was undertaken. As shown in Fig. 1, Ti–Ni shape memory alloy leads (called ‘effectors’ hereafter) whose initial curvature (curvature in memory) was  $\kappa_0 (= 1/R_0)$  and a matrix whose curvature was  $\kappa (= 1/R)$  were compositized and the constraint was released thereafter. The ERC curvatures,  $\kappa_1 (= 1/R_1)$  and  $\kappa_2 (= 1/R_2)$ , at low and high temperatures, respectively, are expressed as [1–4]

$$\kappa_1 = \kappa_0 + \frac{E_{ml} I_m (\kappa - \kappa_0)}{E_{el} I_e + E_{ml} I_m}, \tag{1}$$

$$\kappa_2 = \kappa_0 + \frac{E_{mh} I_m (\kappa - \kappa_0)}{E_{eh} I_e + E_{mh} I_m}, \tag{2}$$

where  $E_{ml}$  and  $E_{mh}$  are the Young’s moduli of the matrix at low temperature and at high temperature, respectively,  $E_{el}$  and  $E_{eh}$  are the Young’s moduli of the effector at

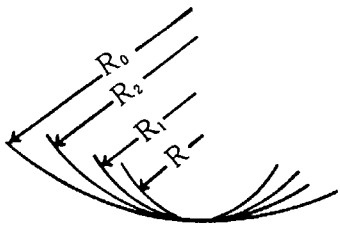


Figure 1. Flexural responses of environmentally responsive composites.



low temperature and at high temperature, respectively, and  $I_m$  and  $I_e$  are the moment of inertia of the matrix and the effector, respectively. The values of both  $\kappa_1$  and  $\kappa_2$  can be controlled by properly choosing the values in the right hand sides of equations (1) and (2). It is easier to control the value of flexural rigidity ( $EI$ ) for the matrix than for the effector by selecting the thickness and the width to tailor the moment of inertia of the matrix. In this paper,  $\kappa_1$  and  $\kappa_2$  are to be controlled by selecting the material properties,  $E_m$  and  $I_m$ , and the curvature,  $\kappa$ , of the matrix when the material properties of the effector are given. By solving for  $E_{ml}I_m$  and  $\kappa$  in equations (1) and (2) by setting  $(E_{eh}I_e)/(E_{el}I_e) = p$ ,  $(E_{mh}I_m)/(E_{ml}I_m) = q$ , the following expression can be obtained:

$$E_{ml}I_m = \frac{qE_{el}I_e(\kappa_0 - \kappa_1) - pE_{el}I_e(\kappa_0 - \kappa_2)}{q(\kappa_1 - \kappa_2)}, \quad (3)$$

$$\kappa = \kappa_1 + \frac{q(\kappa_1 - \kappa_2)(\kappa_1 - \kappa_0)}{q(\kappa_0 - \kappa_1) - p(\kappa_0 - \kappa_2)}. \quad (4)$$

Because  $q = 1$  in the temperature range where the matrix elastic modulus remains constant, equations (3) and (4) become

$$E_{ml}I_m = E_mI_m = \frac{E_{el}I_e(\kappa_0 - \kappa_1) - pE_{el}I_e(\kappa_0 - \kappa_2)}{\kappa_1 - \kappa_2}, \quad (5)$$

$$\kappa = \kappa_1 + \frac{(\kappa_1 - \kappa_2)(\kappa_1 - \kappa_0)}{(\kappa_0 - \kappa_1) - p(\kappa_0 - \kappa_2)}. \quad (6)$$

The responsive shape of ERC can be controlled by first specifying the values of the ERC curvatures,  $\kappa_1$  and  $\kappa_2$ , at low and high temperatures, respectively, and by compositizing a matrix with the flexural rigidity,  $E_mI_m$ , and the initial curvature,  $\kappa$ , with an effector by specifying the design values for the initial curvature,  $\kappa_0$ , flexural rigidity,  $E_{el}I_e$ , and specific flexural rigidity,  $p$ .

### 3. CONSTITUENT MATERIALS AND ERC SPECIMENS

#### 3.1. Constituent materials characteristics

Ti–Ni shape memory alloys, KSM45 (wire radius of 0.352 mm  $\varnothing$ , shape recovery temperature,  $A_s = 48^\circ\text{C}$ ,  $A_f = 61^\circ\text{C}$ ) manufactured by Kanto Special Steel Inc. were used as the effector. Heat treatment for shape memory of the effector was carried out at  $490^\circ\text{C}$  for 30 min with water rapid cooling to make straight line-shape (initial curvature,  $\kappa_0 = 0$ ) memory. The flexural rigidity at low temperature ( $< A_s$ ) and at high temperature ( $> A_f$ ) was obtained by a three point bending test of a beam with a span of 30 mm. The values of flexural rigidity at low and high temperatures were  $E_{el}I_e = 10.2 \text{ N mm}^2$  (1.04 kgf mm<sup>2</sup>),  $E_{eh}I_e = 42.6 \text{ N mm}^2$  (4.34 kgf mm<sup>2</sup>), respectively, and consequently, the ratio of  $EI$  at high temperature to that at low



temperatures was  $(E_{ch}I_e)/(E_{el}I_e) = 4.17$ . The matrix used was CF RTP (carbon fiber reinforced thermoplastics prepregs, product name: APC-2) manufactured by ICI and was thermally processed at 440°C for 60 min in an electric furnace to be molded with the design curvature. The thickness of CF RTP after molding was 0.15 mm and the elastic modulus was 111 kN/mm<sup>2</sup> (11 300 kgf/mm<sup>2</sup>). As an adhesive or holding material, RTV resin (manufactured by Yokohama Rubber, product name: Hamataito) was used to compositize the matrix and the effector. The elastic modulus of the RTV resin remained almost constant as 1.99 N/mm<sup>2</sup> (0.203 kgf/mm<sup>2</sup>) over the temperature range of ERC (room temperature ~ 65°C). Equations (5) and (6) can be used in the following computation because the elastic moduli of both the CF RTP and RTV resin were almost constant over the temperature change range of 20°C ~ 65°C and the flexural rigidity ratio,  $q$ , of the matrix at high and low temperatures was 1.

3.2. Fabrication of ERC specimens

In order to control the responsive shape of ERC, a matrix can be fabricated in such a way that  $E_mI_m$  and  $\kappa$  are computed from the design values of  $\kappa_1$  and  $\kappa_2$  of ERC as well as the given values for the effector using equations (5) and (6). As shown in Fig. 2, an ERC specimen of kanappe type was fabricated. Five types of specimens were fabricated in such a way that the central angle of the open part of each specimen was given by Table 1 when the perimeter of each specimen was kept at 94.2 mm. This value was chosen based on a specimen that had the internal radius of curvature of 15 mm and became ring-shaped at low temperature (0 open part) (specimen symbol: CA1 and CA2). Table 2 shows the flexural rigidity,  $E_mI_m$ , and the initial curvature,  $\kappa$ , of the matrix calculated from equations (5) and (6). In order to mold the CF RTP used as the matrix to the calculated initial curvature, a cylindrical jig made of steel having the same curvature as the matrix was fabricated and CF RTP was wound around the jig, fixed and molded. The molding processing was carried out at 440°C for about 60 minutes with water rapid cooling. As the thickness of the CF RTP after molding was 0.15 mm, the width of the matrix was adjusted to the value of the design value of flexural rigidity. As  $E_mI_m$  in equation (5) to compute the flexural rigidity of the matrix was for the flexural rigidity per one effector, it was necessary to make the width of the matrix narrower for the specimens of CA1, CA4 and CA5 in order to attain the design flexural rigidity of the matrix, which made the fabrication extremely difficult. For this reason, the number of effectors was increased and the width of the matrix was widened accordingly.

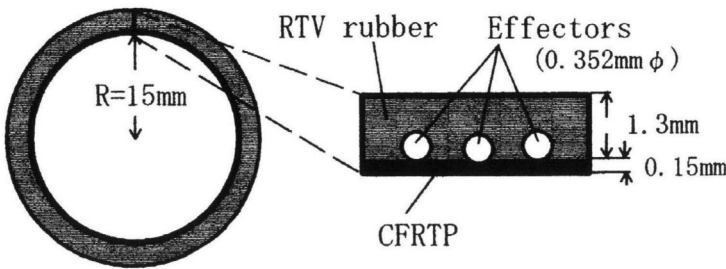
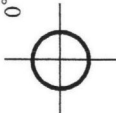
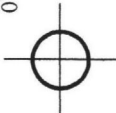
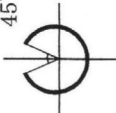
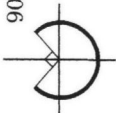
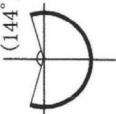
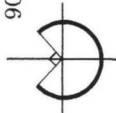
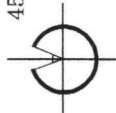
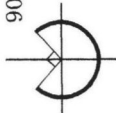
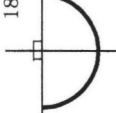
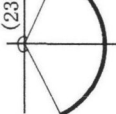


Figure 2. Dimensions and geometry of ERC specimen.



**Table 1.**  
Central angle for open part of ERC specimen (designed value, deg)

Specimen	CA1	CA2	CA3	CA4	CA5
At low temperature	 $\kappa_1 = 1/15.0 \text{ (1/mm)}$	 $\kappa_1 = 1/15.0 \text{ (1/mm)}$	 $\kappa_1 = 1/17.5 \text{ (1/mm)}$	 $\kappa_1 = 1/20.0 \text{ (1/mm)}$	 $\kappa_1 = 1/25.0 \text{ (1/mm)}$
	 $\kappa_2 = 1/20.0 \text{ (1/mm)}$	 $\kappa_2 = 1/17.5 \text{ (1/mm)}$	 $\kappa_2 = 1/20.0 \text{ (1/mm)}$	 $\kappa_2 = 1/30.0 \text{ (1/mm)}$	 $\kappa_2 = 1/41.5 \text{ (1/mm)}$



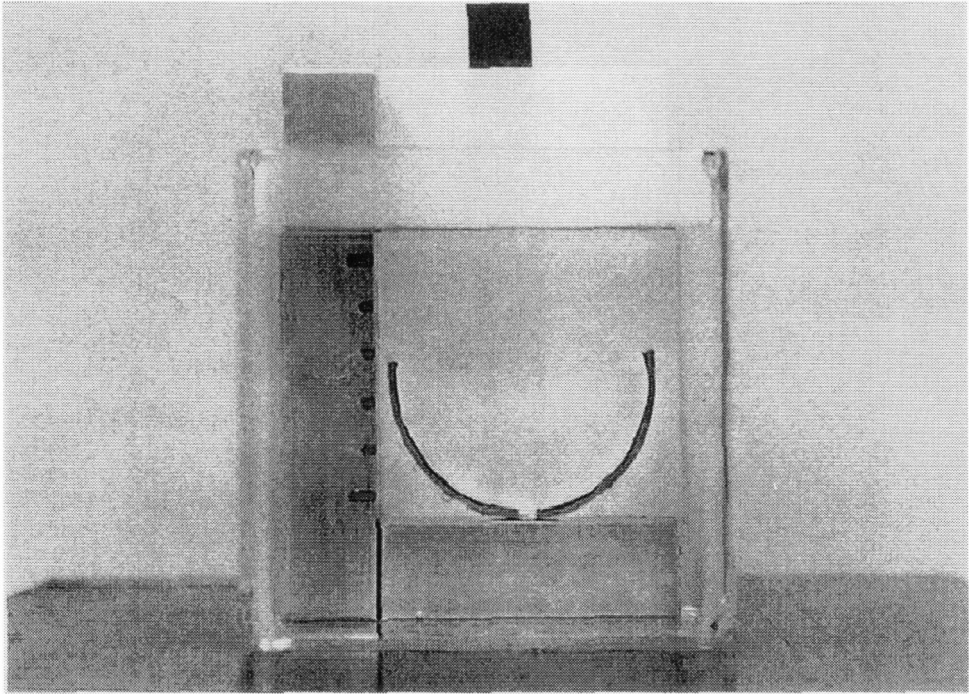


**Figure 3.** Observing apparatus for the responsive shape of ERC specimen (CA4–5) at high temperature.

**Table 2.**

Curvature of ERC specimens were designed and material properties were calculated

Specimen	Curvature of ERC at low temperature, $\kappa_1$ (1/mm)	Curvature of ERC at high temperature, $\kappa_2$ (1/mm)	Flexural rigidity of CF RTP used as matrix of ERC, $E_m I_m$ (N mm <sup>2</sup> ) (kgf mm <sup>2</sup> )		Initial curvature of CF RTP used as matrix of ERC, $\kappa$ (1/mm)	Width of ERC speci- men (mm)	Number of embedded effectors
CA1	1/15	1/20	86.8	(8.85)	1/13.5	6.2	2
CA2	1/15	1/17.5	183	(18.7)	1/14.2	6.6	1
CA3	1/17.5	1/20	216	(22.0)	1/16.7	7.8	1
CA4	1/20	1/30	54.4	(5.55)	1/16.9	5.9	3
CA5	1/30 (1/25)	1/60 (1/41.5)	38.3	(3.96)	1/20.6	5.0	4

As the number of effectors for CA5 was too many for the width of the specimen, this number was reduced to one half for the fabrication purposes and the curvature as the design value was obtained as shown in parenthesis in Table 2. The effector and the matrix were compositized by winding CF RTP around the jig (the curvature was  $\kappa$ ) and by applying a rapid dry adhesive for plastics at several places to press the effectors for temporary holding. RTV resin molded as a sheet with a thickness of 1.3 mm was coated on the surface using the same RTV resin material to make ERC specimens.



#### 4. EXPERIMENT AND ANALYSIS METHOD

Pictures of the ERC specimens at both low and high temperatures were taken and their shapes were measured from the pictures. In order to avoid an image distortion when observed from outside, the specimens and a ruler with 50 mm scaling were placed in a vessel made of plane glass and their pictures were taken from outside. The specimens' pictures at low temperature were taken in air (room temperature at 25°C) and their pictures at high temperature were taken by filling with hot water (60–65°C, heated by an electric heater to maintain the high temperature) and by placing the specimens and the scale together inside after the deformation of the specimens was completed. Care was taken to place the scale and the specimens on the same plane so that the pictures of both the specimens and the scale were at the same magnification ratio. The radii of curvature,  $R$ , of the specimens were obtained by measuring the lengths of  $a$ ,  $b$  and  $s$  in Fig. 4 from the pictures and using equation (7) as (see the Appendix for details)

$$R = \frac{s}{2} \sqrt{\frac{1}{1 - \delta^2}}, \quad \delta = \frac{a^2 + b^2 - s^2}{2ab}. \quad (7)$$

As the value of  $R$  obtained in this equation was the radius of the curvature on the picture, it was multiplied with the ratio of the value measuring the scale on the picture to the actual scale length (50 mm) to be used as the radius of curvature for the experiment specimens.

(Actual radius of curvature)

$$= (\text{Radius of curvature on picture}) \times \frac{(\text{Actual scale length})(50 \text{ mm})}{(\text{Scaling length on picture})}$$

The radius of curvature was measured twice. In the first measurement, the shape change was measured after performing low/high temperature environmental responses for three cycles by warm water soaking after the specimens were fabricated and in the second measurement, the shape change 20 cycles after the fabrication of the specimens was measured. Figure 5 shows examples of the change of responsive shape.

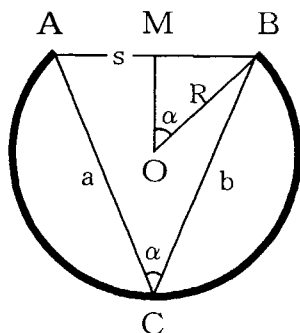


**Figure 4.** Chimerical model for calculating of responsive shape.



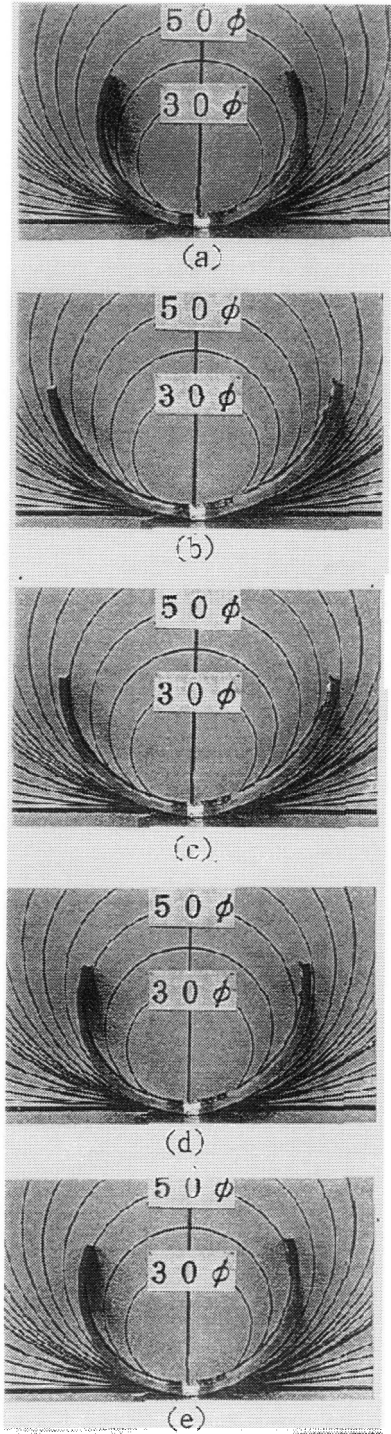


**Figure 5.** Time dependant process of bi-directional shape response for ERC specimens (specimen: CA5-4).



**5. EXPERIMENT RESULT AND DISCUSSION**

Table 3 shows the experimental result for controlling the shape of ERC test specimens. The responsive shapes for each test specimen and at each temperature are shown by the curvatures of the specimens. The test was conducted twice for each in order to observe the influence of response hysteresis. The ratios of the experimental value to the design value at low (room) temperatures were 0.98–1.10 for the first test and

**Table 3.**  
Experimental results of shape control of ERC specimens

Specimen	Curvature of ERC specimens at low temperature, $\kappa_1 (= 1/R_1)$					Curvature of ERC specimens at high temperature, $\kappa_2 (= 1/R_2)$				
	Designed	1st		2nd		Designed	1st		2nd	
	value, $\kappa_{1d}$ (1/mm)	Experimental value, $\kappa_{1e}$ (1/mm)	Ratio $\kappa_{1e}/\kappa_{1d}$	Experimental value, $\kappa_{1e}$ (1/mm)	Ratio $\kappa_{1e}/\kappa_{1d}$	value, $\kappa_{2d}$ (1/mm)	Experimental value, $\kappa_{2e}$ (1/mm)	Ratio $\kappa_{2e}/\kappa_{2d}$	Experimental value, $\kappa_{2e}$ (1/mm)	Ratio $\kappa_{2e}/\kappa_{2d}$
CA1-1	1/15.0	1/15.21	0.99	1/15.20	0.99	1/20.0	1/16.90	1.18	1/17.67	1.13
2		1/15.56	0.96	1/15.43	0.97		1/17.36	1.15	1/17.89	1.12
3		1/15.33	0.98	1/15.06	1.00		1/16.65	1.20	1/17.43	1.15
4		1/15.33	0.98	1/15.16	0.99		1/17.04	1.17	1/17.79	1.12
5		1/15.42	0.97	1/15.36	0.98		1/16.67	1.20	1/17.89	1.12
Mean			0.98		0.98			<b>1.18</b>		1.13
CA2-1	1/15.0	1/15.28	0.98	1/15.03	1.00	1/17.5	1/16.68	1.05	1/16.88	1.04
2		1/15.39	0.97	1/15.03	1.00		1/16.67	1.05	1/16.77	1.04
3		1/15.28	0.98	1/15.50	0.97		1/16.75	1.04	1/17.05	1.03
4		1/15.51	0.97	1/15.33	0.98		1/16.63	1.05	1/16.79	1.04
5		1/14.96	1.00	1/15.04	1.00		1/16.05	1.09	1/15.93	1.10
Mean			0.98		0.99			1.06		1.05
CA3-1	1/17.5	1/17.94	0.98	1/18.31	0.96	1/20.0	1/19.22	1.04	1/20.50	0.98
2		1/17.49	1.00	1/17.81	0.98		1/18.44	1.08	1/19.50	1.03
3		1/17.12	1.02	1/17.31	1.01		1/18.57	1.08	1/18.89	1.06
4		1/17.49	1.00	1/17.81	0.98		1/18.95	1.06	1/19.48	1.03
5		1/17.96	0.97	1/18.24	0.96		1/19.52	1.02	1/19.80	1.01
Mean			0.99		0.98			1.06		1.02
CA4-1	1/20.0	1/18.83	1.06	1/20.12	0.99	1/30.0	1/23.05	1.30	1/27.29	1.10
2		1/18.75	1.07	1/20.18	0.99		1/22.67	1.32	1/27.39	1.10
3		1/18.57	1.08	1/19.62	1.02		1/21.86	1.37	1/25.74	1.17
4		1/19.02	0.05	1/20.59	0.97		1/24.60	1.22	1/27.66	1.08
5		1/19.06	1.05	1/20.36	0.98		1/22.79	1.31	1/28.18	1.06
Mean			1.06		0.99			1.30		1.10
CA5-1	1/25.0	1/22.64	1.10	1/22.58	1.11	1/41.5	1/31.26	1.33	1/34.93	1.19
2		1/22.08	1.13	1/25.38	0.99		1/34.67	1.20	1/41.44	1.00
3		1/22.90	1.09	1/22.64	1.10		1/30.80	1.35	1/32.03	1.30
4		1/22.81	1.10	1/22.76	1.10		1/30.73	1.35	1/33.07	1.25
5		1/23.73	1.05	1/23.52	1.06		1/34.45	1.20	1/38.19	1.09
Mean			1.10		1.07			1.28		1.16



0.98–1.07 for the second test by taking the average over five specimens for each test. These results show good agreement. At high temperatures, the ratios of the experimental value to the design value for curvatures were 1.06–1.30 (first test) and 1.02–1.16 (second test) which indicates that the difference between the theory and the experiment was less than 20% (except for the first test specimens of CA4 and CA5) implying that the theory and the experiment agreed well. However, the ratios of the design value to the experimental value for each specimen in both tests were larger than 1.0, meaning that none of the specimens attained the designed shape. One of the possible reasons for this is because Ti–Ni alloys are in the austenite phase at high temperatures and the so-called ‘plateau phenomenon’ may have taken place where the stress is constant under the progress of strains. It is necessary to examine in more detail the stress–strain relationship at each temperature level and at each phase of Ti–Ni alloys leads. It is not clear why there was so much discrepancy between the experimental values and theoretical values for CA4 and CA5 in the first test. More detailed investigation on the stress–strain relationship for Ti–Ni alloy leads is planned in the future.

The assumption of small elastic deformation in the analysis in Section 2 is now examined. The actual deformation for the specimen, CA4, was the largest as shown in Table 2 and the curvature of the specimen changed from  $1/16.9$  at the time of molding to  $1/30$  at high temperature. In this case, the neutral plane is close to the boundary between the CFRTP and RTV rubber. The maximum strain on the test specimen cross-section is at the external surface (RTV rubber) and its value can be obtained from small deformation elasticity theory as

$$\varepsilon_x = \left( \frac{1}{R'} - \frac{1}{R} \right) Z \quad (8)$$

$$= \left( \frac{1}{30 + 0.15} - \frac{1}{16.9 + 0.15} \right) \times 1.3 = -3.32\%, \quad (9)$$

where  $1/R'$  and  $1/R$  are the curvatures of the neutral surface after and before the deformation, respectively, and  $Z$  is the distance from the neutral surface. At the time of molding, the angle formed by the perimeter of the specimen was changed from  $\alpha = 1.773\pi$  to  $\alpha = \pi$  at high temperature. The strain can be estimated from this as

$$\varepsilon_x = \frac{\pi(30 + 0.15 + 1.3) - 1.773\pi(16.9 + 0.15 + 1.3)}{1.773\pi(16.9 + 0.15 + 1.3)} = -3.32\%. \quad (10)$$

As the latter value estimated from the change in perimeter length of the cross section is the exact value that can be applied from small deformation to large deformation, the fact that the value of the former agrees with this value implies that the assumption of small elastic deformation seems reasonable.



## 6. CONCLUSIONS

The control method of responsive shape necessary for commercialization of environmentally responsive composite materials that use Ti–Ni shape memory alloys and CFRTP was investigated. When the material properties of effectors are given, the curvatures,  $\kappa_1$  and  $\kappa_2$ , at low and high temperatures, respectively, can be chosen as the design variables. The expressions for the material properties of the matrix were derived and the responsive shape of the fabricated specimens were measured based on these values. As a result, the ratios of experimental value/design value (theoretical value) were satisfactory and thus the derived theoretical expressions were verified. Other practically important factors include forces generated at the responsive time and responsive control for multiple types of matrices. These problems will be addressed in the subsequent reports.

## Acknowledgements

Thanks are due to Mr Nobuo Sekino of Kanto Special Steels, Inc. and Mr Satoshi Kitami of Yokohama Rubber, Inc. for technical assistance and in providing constituent materials.

## REFERENCES

1. Yoshida, H. In: *Proc. NIMC-RIMCOF Joint Forum, 'Smart Composite System'*. (1994), pp. 33–41.
2. Yoshida, H. *J. Soc. Rubber Industry, Japan* **67** (10), 105–115 (1994).
3. Yoshida, H. In: *Proc. 39th FRP CON-EX'94 of the Society of Fiber Reinforced Plastic*. Japan (1994), pp. 181–184.
4. Yoshida, H. *Adv. Compos. Mater.* **5** (1), 1–16 (1995).

## APPENDIX

### Computation of radius of curvature, $R$

In Fig. 4,  $A$  and  $B$  are the ends of the specimen opening parts and  $M$  is the middle point of  $AB$ . The lengths of segments,  $AC$ ,  $BC$  and  $AB$ , are denoted as  $a$ ,  $b$  and  $s$ , respectively, and the angle of  $\angle ACB = \angle MOB$  is denoted as  $\alpha$ . By applying the cosine theorem to  $\triangle ACB$ , one obtains

$$s^2 = a^2 + b^2 - 2ab \cos \alpha. \quad (A1)$$

From equation (A1),

$$\cos \alpha = \frac{a^2 + b^2 - s^2}{2ab}. \quad (A2)$$

By knowing the values of  $a$ ,  $b$  and  $s$ , the value of  $\cos \alpha$  can be obtained. Furthermore, as  $BO = R$ ,  $BM = s/2$  and  $OM = R \cos \alpha$ , in  $\triangle BOM$ , the Pythagoras theorem yields

$$R^2 = \left(\frac{s}{2}\right)^2 + (R \cos \alpha)^2. \quad (A3)$$



From equation (A3), one obtains

$$R = \frac{s}{2} \sqrt{\frac{1}{1 - \cos^2 \alpha}}. \tag{A4}$$

By substituting equation (A2) into equation (A4), one obtains

$$R = \frac{s}{2} \sqrt{\frac{1}{1 - \delta^2}}, \tag{A5}$$

where

$$\delta = \frac{a^2 + b^2 - s^2}{2ab}.$$

Thus, the radius of curvature,  $R$ , can be found from equation (A5).